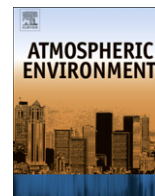


Contents lists available at [SciVerse ScienceDirect](http://www.sciencedirect.com)

# Atmospheric Environment

journal homepage: [www.elsevier.com/locate/atmosenv](http://www.elsevier.com/locate/atmosenv)

## The role of carbon dioxide in emission of ammonia from manure

Sasha D. Hafner\*, Felipe Montes, C. Alan Rotz

USDA-ARS, Pasture Systems and Watershed Management Research Unit, 3702 Curtin Rd., University Park, PA 16802, USA

### ARTICLE INFO

#### Article history:

Received 28 September 2011

Received in revised form

10 January 2012

Accepted 11 January 2012

#### Keywords:

Ammonia emission

Carbon dioxide emission

Manure

Chemical speciation

Mass transfer

Model

### ABSTRACT

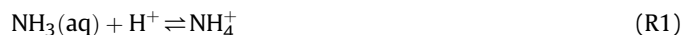
Ammonia emission from manure is a significant loss of fixed N from agricultural systems and contributes to air pollution and ecosystem degradation. Despite the development of numerous mathematical models for predicting ammonia emission, the interactions between CO<sub>2</sub> emission, manure pH, and ammonia emission are not completely understood. Others have recognized that CO<sub>2</sub> emission from manure can increase the surface pH, and so increase the rate of NH<sub>3</sub> emission, but this interaction has not been completely described or quantified. In this work, we present a model of simultaneous NH<sub>3</sub> and CO<sub>2</sub> emission that includes equilibrium acid/base reactions, kinetically-limited CO<sub>2</sub> hydration/dehydration reactions, and diffusive transport. Our model accurately predicted the increase in NH<sub>3</sub> emission from simple solutions due to CO<sub>2</sub> emission, while an equilibrium-only model did not. Model predictions showed that when NH<sub>3</sub> and CO<sub>2</sub> emission occur simultaneously, CO<sub>2</sub> emission generally increases NH<sub>3</sub> emission rate by causing an elevation in surface pH. For thin stagnant layers, this response occurs under a wide range of conditions, although the magnitude of the effect is dependent on manure composition, temperature, surface mass transfer coefficient, and other parameters. Kinetically-limited CO<sub>2</sub> hydration/dehydration reactions moderate this interaction, so equilibrium-based models tend to over-predict NH<sub>3</sub> emission in the absence of significant carbonic anhydrase activity. Predicted emission from deep, mixed manure showed less dependence on CO<sub>2</sub> emission, although higher rates of CO<sub>2</sub> hydration/dehydration increase this effect. Interactions between CO<sub>2</sub> and NH<sub>3</sub> emission influence the effect of model parameters on NH<sub>3</sub> emission and result in some unexpected responses. Future work should clarify the processes controlling CO<sub>2</sub> speciation and transport in manure, including CO<sub>2</sub> minerals, bubble transport, and CO<sub>2</sub> hydration/dehydration rates. Our model can inform the development of simpler models for estimating NH<sub>3</sub> emission, and the design of experiments aimed at quantifying processes that influence NH<sub>3</sub> emission from manure. The effects of CO<sub>2</sub> on NH<sub>3</sub> emission deserve more attention, and both experimental and modeling approaches are needed to understand the interactions that control NH<sub>3</sub> emission.

Published by Elsevier Ltd.

### 1. Introduction

Emission of ammonia (NH<sub>3</sub>) into the atmosphere contributes to atmospheric particulate matter formation, and degradation of terrestrial and aquatic ecosystems (Galloway et al., 2003). In the United States, animal agriculture is thought to contribute about 2 Mg of NH<sub>3</sub> emissions per year, out of total anthropogenic emissions of about 4 Mg (EPA, 2004, 2009). The majority of this NH<sub>3</sub> comes from livestock manure, which is exposed to the atmosphere in barns, during storage, and through field application. In addition to its environmental effects, NH<sub>3</sub> emission from agricultural systems is a loss of valuable fixed N.

Manure NH<sub>3</sub> is formed primarily from the hydrolysis of urea, which cattle excrete in urine. The rate of hydrolysis may limit NH<sub>3</sub> emission within the first few hours after excretion. This work focuses on volatilization in the period after urea hydrolysis is completed, which may last for months when manure is stored. In manure, total NH<sub>3</sub> exists primarily as two species, free ammonia, NH<sub>3</sub> (aq), and ammonium, NH<sub>4</sub><sup>+</sup>, which exist in pH-dependent equilibrium:



Since NH<sub>3</sub> (aq) is volatile and NH<sub>4</sub><sup>+</sup> is not, pH has a significant effect on NH<sub>3</sub> emission rates.

Manure is a moderately concentrated solution with pH largely controlled by NH<sub>3</sub> and CO<sub>2</sub> (Sommer and Husted, 1995a; Hafner and Bisogni, 2009). Production or loss of CO<sub>2</sub> and NH<sub>3</sub> therefore influences manure pH, and may create variation in pH over space and time. Emission of CO<sub>2</sub> is generally greater than that of NH<sub>3</sub> due to

\* Corresponding author. Current address: USDA-ARS, 10300 Baltimore Ave., Building 308, Rm. 113, Beltsville, MD 20705, USA.

E-mail addresses: [sasha.hafner@ars.usda.gov](mailto:sasha.hafner@ars.usda.gov), [sdh11@cornell.edu](mailto:sdh11@cornell.edu) (S.D. Hafner).

a much lower solubility (more than 1000-fold). Therefore, CO<sub>2</sub> emission would be expected to generally lead to an increase in NH<sub>3</sub> emission rate during simultaneous emission of CO<sub>2</sub> and NH<sub>3</sub>.

These interactions may play a significant role in controlling NH<sub>3</sub> emission. Measurements have shown that the surface pH of manure increases following exposure to moving air, in some cases >1 pH unit (Sommer et al., 1991; Chaoui et al., 2009; Ni et al., 2009), presumably due to CO<sub>2</sub> emission. Models of NH<sub>3</sub> emission generally incorporate the effect of manure pH on emission rate, but do not predict pH. An incomplete understanding of changes in pH limits the accuracy of NH<sub>3</sub> emission models (Genermont and Cellier, 1997; Sommer et al., 2003).

Attempts have been made to simulate interactions among NH<sub>3</sub> and CO<sub>2</sub> emission and solution pH. Ni et al. (2000) presented a transient model for NH<sub>3</sub> emission that included an empirical relationship for the effect of increasing surface pH. Blanes-Vidal et al. (Blanes-Vidal et al., 2009, 2010; Blanes-Vidal and Nadimi, 2011) extended an earlier steady-state two-film model (Blunden et al., 2008) by including CO<sub>2</sub> and NH<sub>3</sub> emission. Their model included the effect of CO<sub>2</sub> emission on manure pH through equilibrium-based reactions, and predicted an elevation in surface pH and NH<sub>3</sub> flux due to CO<sub>2</sub> emission, which is qualitatively consistent with measurements. Since CO<sub>2</sub> hydration/dehydration reactions are relatively slow (Kern, 1960), the model may overestimate the effect of CO<sub>2</sub> emission. And, as with most two-film models, concentration gradients within the aqueous film were assumed to be linear, which limits the ability of the model to predict rapid changes.

Earlier, Kirk and Rachhpal-Singh (1992) presented a more complete steady-state model for simultaneous CO<sub>2</sub> and NH<sub>3</sub> emission from water in rice fields. Their model included kinetically-controlled CO<sub>2</sub> hydration/dehydration reactions, along with equilibrium speciation and diffusive transport (Kirk and Rachhpal-Singh, 1992). These researchers predicted that CO<sub>2</sub> and NH<sub>3</sub> emission can generate a pH gradient in the aqueous film, and they demonstrated a substantial effect of CO<sub>2</sub> hydration/dehydration rates on this gradient and on NH<sub>3</sub> emission rates. In this work, we present a model similar to that presented by Kirk and Rachhpal-Singh (1992), which we used to explore interactions among CO<sub>2</sub> emission, manure pH, and NH<sub>3</sub> emission.

## 2. Methods

### 2.1. Model description

Our model included simultaneous emission of NH<sub>3</sub> and CO<sub>2</sub> from manure, aqueous-phase acid/base and hydration/dehydration reactions, and diffusive transport within manure, for transient or steady-state conditions. In dairy manure, pH is generally determined by CO<sub>2</sub>, NH<sub>3</sub>, volatile fatty acids (primarily acetic acid), Na, K, and Cl (Sommer and Husted, 1995a). These six solutes were included in our model. Calcium and Mg are also present at high concentrations in manure, but are largely precipitated in mineral phases (Sommer and Husted, 1995b; Gungor and Karthikeyan, 2008) where they do not greatly influence solution speciation (although formation and dissolution of these minerals will influence speciation).

Carbon dioxide (CO<sub>2</sub>) and free ammonia (NH<sub>3</sub>) were the only compounds that volatilize in our model. Although acetic acid is also volatile, calculated emission rates are much lower than NH<sub>3</sub> and CO<sub>2</sub>, due primarily to high solubility. Other gases, such as methane and nitrous oxide, may also be emitted from manure, but these compounds are produced more slowly, and do not directly participate in acid/base reactions. Volatilization of CO<sub>2</sub> and NH<sub>3</sub> was modeled using a mass transfer coefficient approach, Eq. (1), where  $j_i$  = flux of  $i$  ( $i = \text{CO}_2$  or  $\text{NH}_3$ ) from the manure surface (mol m<sup>-2</sup> s<sup>-1</sup>),  $h_{m,i}$  = mass transfer coefficient of  $i$  (m s<sup>-1</sup>),

$a_i$  = activity of species  $i$  at the manure surface (molal scale, mol kg<sup>-1</sup>),  $H_i$  = Henry's law constant for  $i$  (aq:g, m<sup>3</sup> kg<sup>-1</sup>), and  $c_{i,\infty}$  = gas-phase concentration of  $i$  in ambient air (mol m<sup>-3</sup>).

$$j_i = h_{m,i} \left( \frac{a_i}{H_i} - c_{i,\infty} \right) \quad (1)$$

The value of the mass transfer coefficient was set for either NH<sub>3</sub> or CO<sub>2</sub> and then calculated for the other by assuming it to be inversely proportional to the square root of molecular weight (Liss and Slater, 1974). Expressions for calculating Henry's law constants as a function of temperature were recalculated from Clegg and Brimblecombe (1989) for NH<sub>3</sub> and Plummer and Busenberg (1982) for CO<sub>2</sub>:

$$\log K_{H_{\text{NH}_3}} = -3.51645 - 0.00136T + \frac{1701.34805}{T} \quad (2)$$

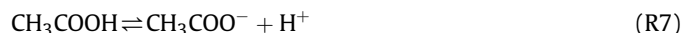
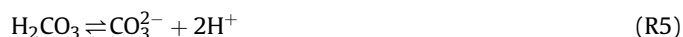
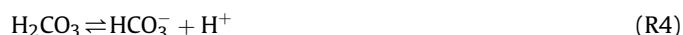
$$\log K_{H_{\text{CO}_2}} = 108.38578 + 0.01985T + \frac{-6919.530}{T} - 40.45154 \log T + \frac{669365}{T^2} \quad (3)$$

where  $K_{H_i}$  = Henry's law constant in mol kg<sup>-1</sup> atm<sup>-1</sup> (which can be converted to m<sup>3</sup> kg<sup>-1</sup> by multiplying by  $RT$ , where  $R$  = universal gas constant, and  $T$  = temperature (K)).

In solution, dissolved CO<sub>2</sub> is hydrated to form carbonic acid (H<sub>2</sub>CO<sub>3</sub>), through reactions (R2) and (R3), with (R2) dominating below pH 10. Reactions (R2) and (R3) are relatively slow, with a half-life of CO<sub>2</sub> (aq) of about 25 s at 25 °C and pH 7 (Kern, 1960).



In solution, H<sub>2</sub>CO<sub>3</sub> exists in equilibrium with bicarbonate, HCO<sub>3</sub><sup>-</sup>, and carbonate, CO<sub>3</sub><sup>2-</sup>. Reactions (R4) through (R8) were included in our model, and were at equilibrium at all times and locations.



Expressions for calculating equilibrium constants as a function of temperature were based on Plummer and Busenberg (1982) for CO<sub>2</sub>, Clegg and Whitfield (1995) for NH<sub>3</sub>, and Martell et al. (2004) for other reactions. For reactions (R4) and (R5), respectively,

$$\log K_{\text{HCO}_3} = -353.5305 - 0.060920T + \frac{21834.37}{T} + 126.8339 \log T - \frac{1684915}{T^2} \quad (4)$$

$$\log K_{\text{CO}_3} = -461.4176 - 0.093448T + \frac{26986.16}{T} + 165.7595 \log T - \frac{2248629}{T^2} \quad (5)$$

where  $T$  = temperature in K. For ammonia, reaction (R6),

$$\log K_{\text{NH}_3} = 0.09046 + \frac{2729.31}{T} \quad (6)$$

For acetic acid, reaction (R7),

$$\log K_{\text{CH}_3\text{COOH}} = -4.8288 + \frac{21.42}{T} \quad (7)$$

And lastly, for water, reaction (R8),

$$\log K_w = -4.2192 - \frac{2915.16}{T} \quad (8)$$

The second-order rate constant for reaction (R2) in the forward direction ( $k_1$ ) and the first-order rate constant for reaction (R3) in the reverse direction ( $k_{-2}$ ) were based on Welch et al. (1969),

$$\log k_1 = 12.0657 - \frac{4018.09}{T} \quad (9)$$

$$\log k_{-2} = 14.8809 - \frac{5524.23}{T} \quad (10)$$

Expressions for the first-order rate constant for reaction (R2) in the reverse direction ( $k_{-1}$ ) and second-order rate constant for reaction (R3) in the forward direction ( $k_2$ ) were derived from Eqs. (9) and (10) and the relevant equilibrium constants to maintain consistency with Plummer and Busenberg's (1982) model:

$$\log k_{-1} = 14.8438 - \frac{4018.09}{T} \quad (11)$$

$$\log k_2 = -337.2083 - 0.060920T + \frac{19225.30}{T} + 126.8339 \log T - \frac{1684915}{T^2} \quad (12)$$

Activity coefficients were calculated using the extended Debye–Hückel equation (Zemaitis, 1986) (see the Supplementary material for details).

Diffusion of solutes (e.g., total  $\text{CO}_2$ , total  $\text{NH}_3$ ) was included using Fick's second law, Eq. (13), where  $j_s$  = diffusive flux of solute  $s$  ( $\text{mol m}^{-2} \text{s}^{-1}$ ),  $D$  = diffusivity in manure ( $\text{m}^2 \text{s}^{-1}$ ),  $c_s$  = total concentration of solute  $s$  (including all species) in manure ( $\text{mol m}^{-3}$ ), and  $z$  = distance from exposed manure surface (m). (We assumed that the mixture velocity was zero.) The density of water within manure was fixed at  $1000 \text{ kg m}^{-3}$ .

$$j_s = -D \frac{dc_s}{dz} \quad (13)$$

Simulating diffusion based on total concentrations is equivalent to simulating species diffusion with a single diffusivity for all species. Since some differences in diffusivity exist, this represents a simplification.

This system of equations was solved using the method of lines (Schiesser, 1991). The spatial dimension was discretized and the resulting set of ordinary differential equations for each layer were solved using the package 'deSolve' in R (R Development Core Team, 2010). The upper  $50 \mu\text{m}$  was divided into  $10 \mu\text{m}$  layers, followed by five  $100 \mu\text{m}$  layers, and the remaining layers were about  $1 \text{ mm}$  thick. Preliminary simulations showed that this configuration resulted in emission predictions within 2% of a configuration consisting of only  $10 \mu\text{m}$  layers, but required much less time for

execution. Simulated emission from a  $10 \mu\text{m}$  configuration was very similar (<2% difference) to results from a simulation with  $1 \mu\text{m}$  layers. At each time step, solution speciation was calculated, treating  $\text{CO}_2$  (aq) as a distinct component from other  $\text{CO}_2$  species. Explicit expressions were used to calculate species concentrations as a function of pH (Supplementary material), and were used along with an  $\text{H}^+$  balance to solve for pH using a one-dimensional optimization algorithm ('optimize' function in R).

Our model did not include all interactions that may play a role in  $\text{NH}_3$  emission from manure. We use an ion association approach to predict speciation, with activity coefficients based on the extended Debye–Hückel equation. This approach becomes inaccurate at high solute concentrations, but a comparison between it and the more comprehensive ion interaction (Pitzer) approach showed that the former is probably accurate for manure (Hafner and Bisogni, 2009). We also ignore organic matter in our model, while some  $\text{NH}_4^+$  is probably absorbed to particulate material and complexed with dissolved organic matter. Limited measurements of anaerobically-digested manure suggest that absorbed  $\text{NH}_4^+$  is minor (Hafner et al., 2006), and comparison between measured and predicted  $\text{NH}_3$  activity in manure digesters suggests that complexation of  $\text{NH}_4^+$  is not significant (Hafner and Bisogni, 2009). Therefore, our speciation approach should be relatively accurate. In our model, simplifications were also made in physical processes. Where mixing occurs, solutes are transferred much more rapidly than by diffusion. Transport of  $\text{CO}_2$  by biogas bubbles to a surface film may be significant, and such bubbles also mix the solution (Ro et al., 2008; Ni et al., 2009). Surface drying or bubbling can lead to the formation of a crust at the surface. Where these processes are important, our model represents a limiting case. In other cases, such as a thin layer of manure, our model probably includes all significant processes.

## 2.2. Experimental methods

We measured ammonia emission from defined solutions in order to evaluate the accuracy of our model. For all trials, 150 mL samples were held in 250 mL straight-sided glass jars (I-Chem, Thermo Fisher Scientific, Fair Lawn, NJ). Stainless steel bulkhead connectors were attached to Teflon-lined lids and sealed using silicone o-rings. Gas flow into the sample jar was routed through a  $90^\circ$  elbow to direct it toward the jar wall just above the sample surface, while a short straight length of tubing was connected to the exhaust bulkhead connector. All tubing downstream of the sample container was teflon. Humidified compressed breathing quality air (Airgas) was passed through the system at a flow rate of about  $300 \text{ mL min}^{-1}$ . Ammonia emission was measured from two types of solutions:  $\text{NH}_4\text{HCO}_3$  (Fisher Scientific, Fair Lawn, NJ; reported assay: 21.55% as  $\text{NH}_3$  (21.54% expected)) and  $\text{NH}_4\text{Cl}$  (Fisher Scientific, Fair Lawn, NJ; reported purity: 99.6%). Both sets of solutions had a total  $\text{NH}_3$  concentration of  $100 \text{ mmol kg}^{-1}$ . The initial pH of pure  $\text{NH}_4\text{HCO}_3$  solutions was 7.8, and NaOH was added to the  $\text{NH}_4\text{Cl}$  solutions at a concentration of  $2.3 \text{ mmol kg}^{-1}$  to result in the same initial pH. To eliminate convective transport within the solutions, low melting point agarose (Gibco-BRL L.M.P. Agarose; Life Technologies, Gaithersburg, MD) was added at a concentration of 0.5%. Solutions were heated to melt the agarose, and salts were added after agarose mixtures had cooled, but before gelling had taken place, to minimize volatilization.

The method described in Hafner et al. (in press) was used to measure cumulative ammonia emission over a 7 h period, with measurements taken once per hour. Two trials were run for each condition, and results were very similar between replicates. To determine the mass transfer coefficient of the system for use in model predictions, mass loss from 150 mL acetone samples was

measured over 20–30 min periods. Acetone samples were stirred, and temperature was measured before and after each trial. For calculations, vapor phase partial pressure of acetone at the liquid surface was taken as the equilibrium partial pressure, which was calculated using the Antoine equation with parameters taken from Linstrom and Mallard (2011).

### 2.3. Description of simulations

We used our model to predict  $\text{NH}_3$  and  $\text{CO}_2$  emission over 24 h under a range of conditions. Parameter values in the 'base' scenario were: ambient  $\text{CO}_2$  partial pressure,  $P_{\text{CO}_2, \infty} = 4.0 \cdot 10^{-4}$  atm; ambient  $\text{NH}_3$  partial pressure,  $P_{\text{NH}_3, \infty} = 0$  atm; temperature = 20 °C; mass transfer coefficient,  $h_{m, \text{NH}_3} = 0.0020$  m  $\text{s}^{-1}$  ( $h_{m, \text{CO}_2} = 0.0012$  m  $\text{s}^{-1}$ ); and solute diffusivity,  $D = 2.0 \cdot 10^{-9}$  m<sup>2</sup>  $\text{s}^{-1}$ . For the simulations described below, most parameters were varied from 0.1- to 10-fold the 'base' value. Temperature was varied from 0 °C to 40 °C. 'Base' scenario solute concentrations were meant to represent typical values for dairy manure (Sommer and Husted, 1995b; Hafner and Bisogni, 2009), and were (in mmol  $\text{kg}^{-1}$ ):  $\text{NH}_3$ , 100;  $\text{CO}_2$ , 100, K, 30; Na, 20; Cl, 30. The 'base' acetic acid concentration was set to 24.2 mmol  $\text{kg}^{-1}$  in order to provide an initial pH of 7.50 at 20 °C. Acetic acid and  $\text{CO}_2$  concentrations were varied separately in additional sets of simulations aimed at assessing the effect of pH change. In other simulations, concentrations of  $\text{CO}_2$  and  $\text{NH}_3$  were separately varied from 0.010 to 1.0 mol  $\text{kg}^{-1}$  while maintaining solution pH at 7.50 by adjusting acetic acid or KOH concentrations as needed. Also,  $\text{CO}_2$  and  $\text{NH}_3$  concentrations were varied while allowing pH to change. In each set of simulations, only a single parameter was varied.

All sets of environmental and manure conditions were applied to two physical conditions: a thin stagnant layer (10 mm in the 'base' scenario) and a deep solution with a stagnant film at the surface (200  $\mu\text{m}$  thickness in the 'base' scenario) and constant solution composition below the film. The second condition was similar to the two-film model that has been applied extensively to gas emission from bodies of water, including manure storage ponds (Liang et al., 2002). Maximum  $\text{NH}_3$  emission in the stagnant layer 'base' scenario was 1.0 mol  $\text{m}^{-2}$  (0.10 mol  $\text{kg}^{-1} \times 1000$  kg  $\text{m}^{-3} \times 0.01$  m).

## 3. Results and discussion

### 3.1. Interactions between $\text{CO}_2$ and $\text{NH}_3$ emission

Model predictions for a 10 mm stagnant layer of manure under the 'base' conditions are shown in Figs. 1 and 2. The model predicted that rapid emission of  $\text{CO}_2$  at the start causes an increase in surface pH, resulting in an increase in  $\text{NH}_3$  flux. Although the magnitude of this effect is dependent on temperature, solution composition, and other parameters (as discussed below), and was not predicted to occur under all conditions, it was predicted to occur under a wide range of conditions.

### 3.2. Comparison with measured emission

Measured  $\text{NH}_3$  emission from defined solutions demonstrated the effect of  $\text{CO}_2$  on  $\text{NH}_3$  emission. As expected,  $\text{NH}_3$  emission measured from  $\text{NH}_4\text{Cl}$  solutions was much lower than emission from  $\text{NH}_4\text{HCO}_3$  solutions, despite identical total  $\text{NH}_3$  concentration and pH (Fig. 3). The complete model accurately predicted the magnitude and trajectory of  $\text{NH}_3$  emission from both types of solutions, although it slightly underpredicted (about 10%) emission from  $\text{NH}_4\text{Cl}$  solutions. Based on model predictions, the difference in emission between the two solutions was caused by an increase in pH near the surface in the  $\text{NH}_4\text{HCO}_3$  solutions due to  $\text{CO}_2$  emission, while no such increase occurred for the  $\text{CO}_2$ -free  $\text{NH}_4\text{Cl}$  solutions.

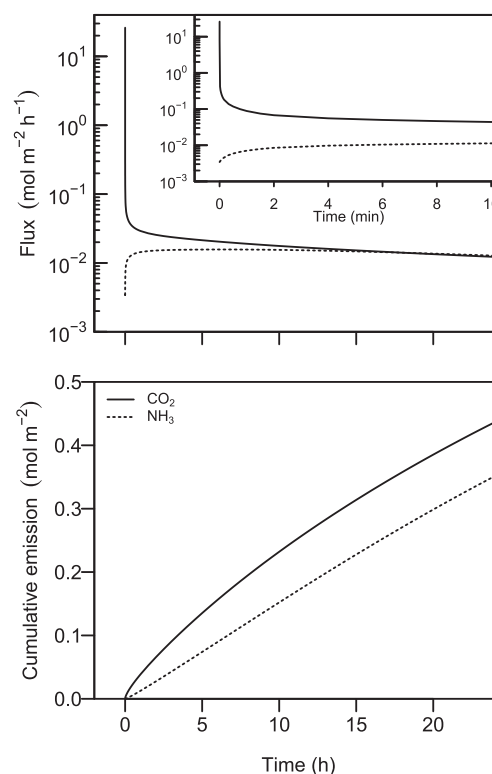


Fig. 1. Predicted  $\text{NH}_3$  and  $\text{CO}_2$  flux (top) and cumulative emission (bottom) from a 10 mm thick stagnant layer of manure at 20 °C over 24 h. The inset in the top panel shows results over the first 10 min.

The model predicted that the surface pH in the  $\text{NH}_4\text{HCO}_3$  solutions increased from 7.79 to 8.22 (values measured in one trial were 7.79 and 8.21), while for the  $\text{NH}_4\text{Cl}$  solutions, the model predicted a decrease in surface pH from 7.82 to 6.87 as  $\text{NH}_3$  was lost. Importantly, results confirm that hydration/dehydration reaction rates moderate the effect of  $\text{CO}_2$  emission on  $\text{NH}_3$  emission; predicted  $\text{NH}_3$  emission from  $\text{NH}_4\text{HCO}_3$  solutions with an equilibrium-based model was much greater than measured emission (Fig. 3). When kinetically-limited reactions are included in the model, slow

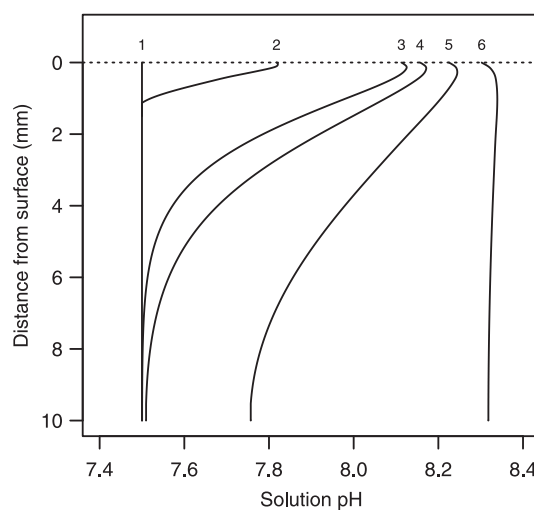
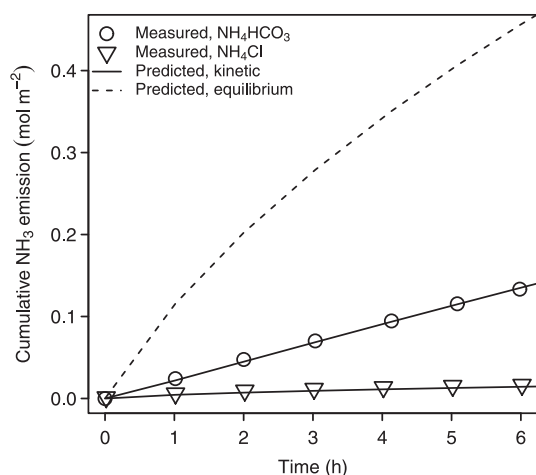


Fig. 2. Solution pH profiles from the simulation shown in Fig. 1. Line labels indicate the following times: 1) initial, 2) 1 min, 3) 30 min, 4) 1 h, 5) 4 h, and 6) 24 h after initial exposure to air.



**Fig. 3.** Measured and predicted  $\text{NH}_3$  emission from  $100 \text{ mmol kg}^{-1} \text{NH}_4\text{HCO}_3$  or  $\text{NH}_4\text{Cl}$ , both with an initial pH of 7.8. Solid lines show predictions from the complete model, with kinetically-limited hydration/dehydration reactions for  $\text{CO}_2$ . The dashed line shows emission from  $\text{NH}_4\text{HCO}_3$  predicted with an equilibrium-based model (kinetic and equilibrium predictions for  $\text{NH}_4\text{Cl}$  are nearly identical). Measurements from duplicate sets of trials were very similar – only those from one set are shown.

reactions limit the rate at which  $\text{H}_2\text{CO}_3$  is dehydrated and volatilized as  $\text{CO}_2$ , and thus the effect of  $\text{CO}_2$  emission on solution pH.

### 3.3. Predicted ammonia emission from thin stagnant layers

Ammonia emission was predicted to be sensitive to all model parameters, with the exception of ambient  $\text{CO}_2$  partial pressure. Although the direction of some of these responses could be predicted with much simpler models, a more complete model provides a more accurate prediction of the magnitude and shape of the responses. The effect of  $\text{CO}_2$  emission on  $\text{NH}_3$  influenced the sensitivity of  $\text{NH}_3$  emission to all other parameters. In general, the effect was to moderate the sensitivity to other parameters.

It is difficult to compare complete 24 h emission trajectories for many different cases to explore the effect of parameter values on  $\text{NH}_3$  emission. Instead, we summarized responses such as that shown in Figs. 1 and 2 (which include five variables and two dimensions) by extracting 1.0 and 24 h cumulative  $\text{NH}_3$  emission and the surface pH elevation (relative to the initial state).

Predicted ammonia emission increased with manure pH, as expected (line 1 in Figs. 4 and 5). However, the response to pH was not as large as simpler models would predict. From pH 6.5 and 8.5, predicted 1 h emission changed by a factor of 4.9, while 24 h emission changed by a factor of 1.8. For constant total  $\text{NH}_3$  and  $\text{CO}_2$  concentrations, the effect of pH was moderated by  $\text{CO}_2$  emission, which declined as pH increased, due to a shift in  $\text{CO}_2$  speciation toward ionic species. At the highest pH values (close to 8.5), surface pH actually declined slightly, due to a high flux of  $\text{NH}_3$ .

Predicted ammonia emission was affected by concentrations of total  $\text{NH}_3$  and total  $\text{CO}_2$ . Higher  $\text{NH}_3$  concentrations increased  $\text{NH}_3$  emission. However,  $\text{NH}_3$  emission was not proportional to the total  $\text{NH}_3$  concentration when initial pH was held constant; the fraction of total  $\text{NH}_3$  lost after 1 and 24 h declined as total  $\text{NH}_3$  increased. Again, this response is due to interactions between surface pH and emission. With the same total  $\text{CO}_2$  concentration and initial pH, a solution with a higher ammonia concentration (and therefore higher  $\text{NH}_3$  emission rate) had less of an increase in surface pH. Conversely, increasing total  $\text{CO}_2$  concentration at a constant  $\text{NH}_3$  concentration and initial pH increased  $\text{NH}_3$  emission, by leading to a greater elevation of surface pH. Increasing  $\text{CO}_2$  concentration while initial concentrations of all other solutes remained constant

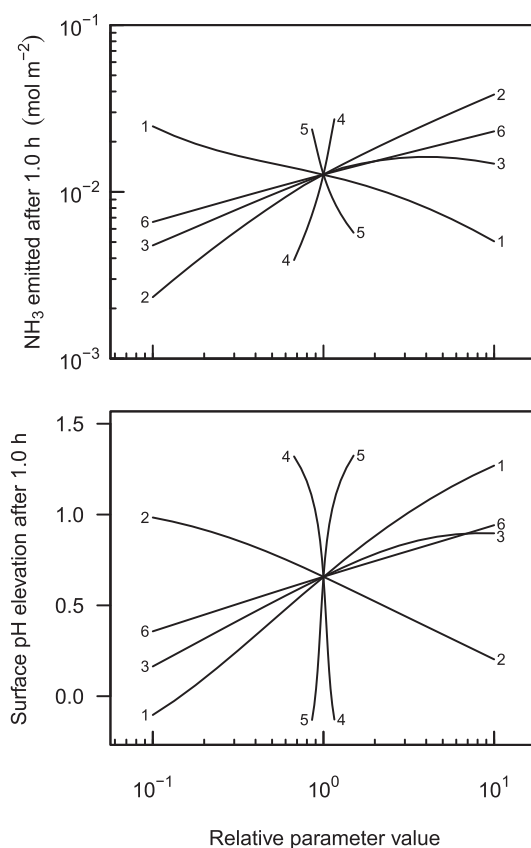


**Fig. 4.** Predicted sensitivity of 1 h cumulative  $\text{NH}_3$  emission (top) and 1 h surface pH elevation (bottom) to model parameter values for a thin stagnant layer of manure. Numbers indicate which parameter was varied: 1) pH (expressed as  $\text{H}^+$  activity); 2) total  $\text{NH}_3$ , initial pH fixed at 7.50; 3) total  $\text{CO}_2$ , initial pH fixed at 7.50; 4) total  $\text{NH}_3$ , with initial concentrations of other solutes fixed, initial pH allowed to vary; 5) total  $\text{CO}_2$ , with initial concentrations of other solutes fixed, initial pH allowed to vary; 6) kinetic rates. A relative parameter value of 1.0 is the 'base' scenario.

resulted in a decrease in manure pH and a reduction in  $\text{NH}_3$  emission, despite a greater elevation in surface pH (line 5 in Figs. 4 and 5). Increasing initial  $\text{NH}_3$  concentration while all initial concentrations of all other solutes remained constant increased manure pH and absolute and relative  $\text{NH}_3$  emission, despite reducing surface pH elevation (line 4 in Figs. 4 and 5).

As demonstrated in the emission measurements, the rate of  $\text{CO}_2$  hydration/dehydration also affects  $\text{NH}_3$  emission (line 6 in Figs. 4 and 5). Higher reaction rates led to higher emission rates of  $\text{CO}_2$  and greater elevation of surface pH, which led to higher rates of  $\text{NH}_3$  emission. A 100-fold change in reaction rates more than doubled 1 and 24 h cumulative  $\text{NH}_3$  emission. (Rates can be elevated by carbonic anhydrase, which is discussed below.)

Model predictions confirmed that both temperature and air movement affect  $\text{NH}_3$  emission (lines 7 and 8 in Figs. 6 and 7). As expected,  $\text{NH}_3$  emission increased with temperature. This response was due to increases in ammonia volatility and the dissociation constant of  $\text{NH}_4^+$  with temperature. The rate of  $\text{H}_2\text{CO}_3$  dehydration also increases with temperature, resulting in high  $\text{CO}_2$  emission rates that maintained high pH and high  $\text{NH}_3$  emission at higher temperatures. Therefore, emission of  $\text{CO}_2$  contributes to a greater sensitivity of  $\text{NH}_3$  emission to changes in temperature. (Note that for the fixed solution composition used, initial pH decreased from 7.75 at  $0^\circ\text{C}$  to 7.31 at  $40^\circ\text{C}$ .) Ammonia emission was also positively related to the mass transfer coefficient. In this case, however, the elevation in surface pH declined as the parameter value increased

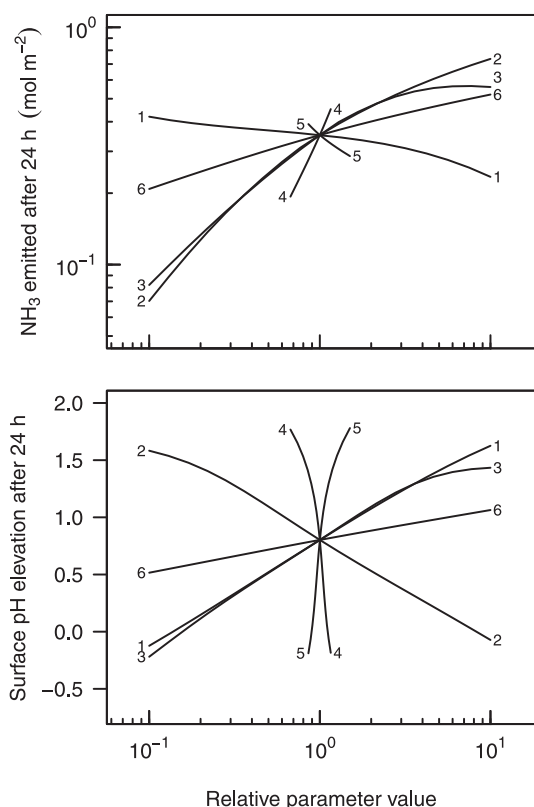


**Fig. 5.** Predicted sensitivity of 24 h cumulative  $\text{NH}_3$  emission (top) and surface pH elevation (bottom) to model parameter values for a thin stagnant layer of manure. Line labels are as in Fig. 4.

due in part to a greater increase in  $\text{NH}_3$  emission than  $\text{CO}_2$  emission (reflecting differences in volatility). Therefore,  $\text{CO}_2$  emission and the resulting elevation of surface pH moderated the effect of an increasing mass transfer coefficient.

Over short periods of time,  $\text{NH}_3$  emission may be higher from thin layers than from thicker layers (line 9 in Fig. 6), due to the effect of  $\text{CO}_2$  emission. This response is due to the increase in the quantity of  $\text{CO}_2$  available for buffering with an increase in thickness. Based on our simulations,  $\text{CO}_2$  emission rate is initially independent of layer thickness. As  $\text{CO}_2$  emission takes place and surface pH increases, thicker layers provide a greater capacity to buffer pH changes through diffusion of  $\text{CO}_2$  species. Surface pH in a thin layer will therefore increase more rapidly than in a thick layer. Ultimately,  $\text{NH}_3$  emission from thick layers exceeds emission from thin layers, simply because thin layers of manure contain less  $\text{NH}_3$  than thick layers (Fig. 7).

The presentation of results from model predictions in Figs. 4–7 provide only a partial image of simulated emission, since cumulative emission at only two times is shown. Also, the scenarios explored in this sensitivity analysis do not encompass all the possible responses that may occur, given reasonable environmental conditions and solution composition. For example, the effect of changes in the rate of kinetically-limited reactions would be greater at lower temperatures. For some parameter value combinations, changes in surface pH and emission rates could be much larger, e.g., with high initial pH, high  $\text{NH}_3$  concentration, low  $\text{CO}_2$  concentration, and high  $h_m$ , a large decline in surface pH would result.

### 3.4. Ammonia emission from mixed manure

The effect of parameter values on  $\text{NH}_3$  emission from mixed manure with a thin stagnant surface film and constant concentrations in the bulk layer showed responses that were qualitatively

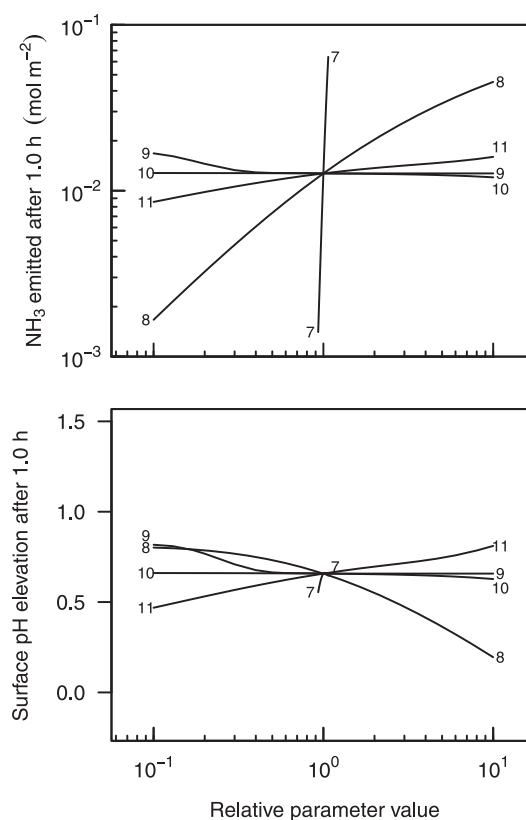


**Fig. 6.** Predicted sensitivity of 1 h cumulative  $\text{NH}_3$  emission (top) and surface pH elevation (bottom) to model parameter values for a thin stagnant layer of manure. Numbers indicate which parameter was varied: 7) temperature (expressed in K), 8) mass transfer coefficient, 9) layer thickness, 10) ambient partial pressure of  $\text{CO}_2$ , 11) solute diffusivity.

similar to those for thin stagnant layers, but with a smaller effect of  $\text{CO}_2$  emission, and greater sensitivity to most parameters (Figs. 8 and 9). Surface elevation of pH was generally much lower in the mixed case, due to buffering by the bulk solution, which provided an infinite pool of  $\text{CO}_2$ . Predicted steady-state pH elevation was  $<0.2$  pH units for the 'base' scenario.

The predicted direction of steady-state  $\text{NH}_3$  flux to parameter changes was generally as expected: flux increased with pH, total  $\text{NH}_3$ , and the mass transfer coefficient, and decreased with total  $\text{CO}_2$ . The more limited effect of  $\text{CO}_2$  emission from the well-mixed case led to a greater sensitivity of  $\text{NH}_3$  to most model parameters. This included pH, total  $\text{NH}_3$  and  $\text{CO}_2$  (with fixed or floating initial pH), mass transfer coefficient, and stagnant film thickness.

Since model predictions indicated that buffering by diffusing solutes plays an important role in moderating  $\text{NH}_3$  emission, steady-state flux was more sensitive to diffusivity than in a thin stagnant layer. Increasing diffusivity caused a reduction in  $\text{NH}_3$  flux, due to the importance of pH buffering by diffusing  $\text{CO}_2$  species. Differences in diffusivity among species, which would require a more sophisticated approach to simulating diffusion, may also affect  $\text{NH}_3$  emission. Because resistance to diffusion from the bulk layer increases as the stagnant film thickness increases, surface pH elevation was predicted to increase as this thickness increased. This elevation in surface pH had a greater effect on  $\text{NH}_3$  emission than did the greater resistance to diffusing  $\text{NH}_3$  species, and so  $\text{NH}_3$  emission increased with thickness. This result implies that mixing will reduce  $\text{NH}_3$  flux, and the model predicts that the effect continues beyond the range shown in Fig. 9; predicted 1 d emission

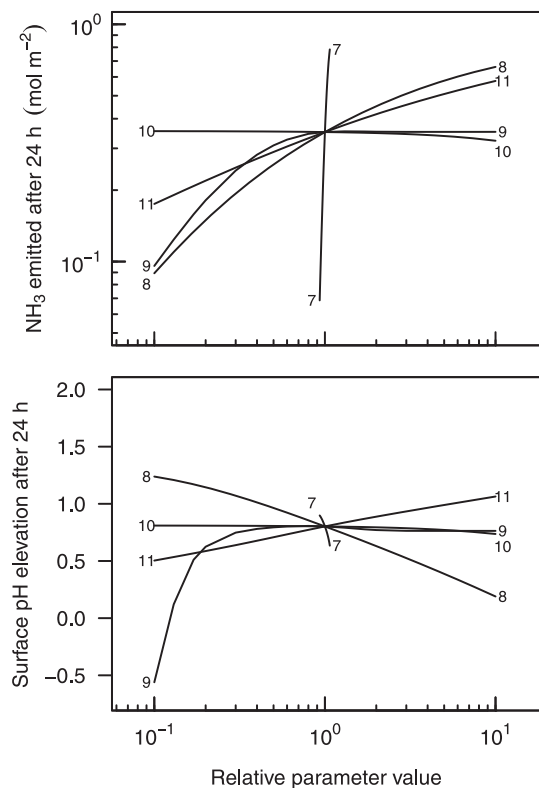


**Fig. 7.** Predicted sensitivity of 24 h cumulative  $\text{NH}_3$  emission (top) and surface pH elevation (bottom) to model parameter values for a thin stagnant layer of manure. Line labels are as in Fig. 6.

from a stagnant layer 100 mm deep was >3-fold emission from the 'base' mixed scenario.

### 3.5. Implications

The processes included in our model are well-understood, and parameter values have been accurately quantified. The only significant simplification is the handling of diffusion, which does not allow for different diffusivities among species. The model is accurate for simple solutions (Fig. 3). As described above, additional processes may be important in cattle manure, and in these cases our model would not provide a complete description. Our model is not aimed at predicting on-farm  $\text{NH}_3$  emissions (although it may provide accurate estimates in some cases), but rather is useful as a tool for better understanding the processes that control ammonia emission from manure.

Measurements of  $\text{NH}_3$  and  $\text{CO}_2$  emission from manure under well-defined conditions could be used to compare the importance of the processes included in our model with other processes. Unfortunately, we are not aware of such measurements. Nonetheless, two studies present incomplete data that are consistent with model predictions. Ni et al. (2009) measured emission from 104 L of swine manure (about 5% total solids) in a 1.2 m column (manure depth of 92 cm). Clean air was flushed through the column headspace. After incomplete mixing of the manure by shaking, exhaust  $\text{NH}_3$  concentration declined, followed by an increase, and then a leveling-off after about 30 min (Fig. 6 in Ni et al., 2009). Conversely,  $\text{CO}_2$  concentration spiked quickly after shaking, and then declined over the next 60 min. These responses are consistent with our model predictions. The decline in  $\text{NH}_3$  can be explained by a sudden drop in surface pH due to transport of  $\text{CO}_2$  to the surface

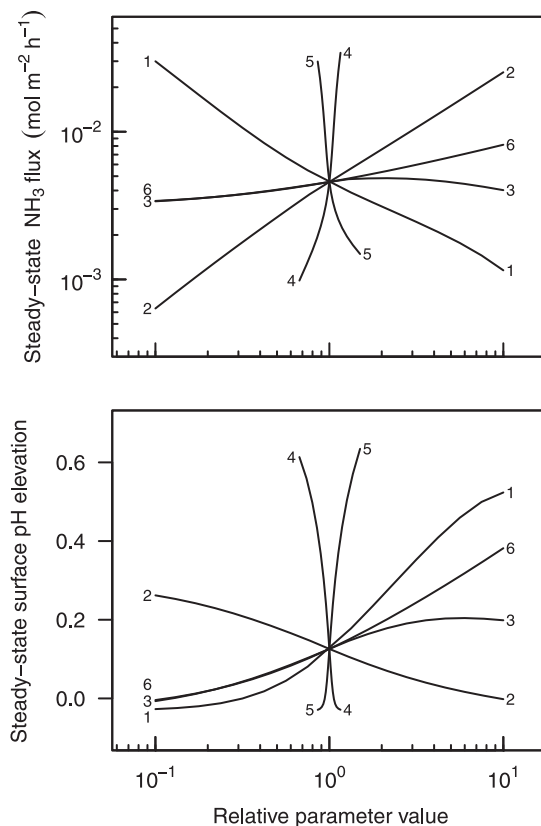


**Fig. 8.** Predicted sensitivity of steady-state  $\text{NH}_3$  flux (top) and surface pH elevation (bottom) to model parameters for manure with a stagnant film at the surface and a bulk solution with a constant composition. Line labels are as in Fig. 4.

by mixing. The subsequent increase in  $\text{NH}_3$  can be explained by the increase in surface pH that followed, as  $\text{CO}_2$  emission resulted in depletion.

Chaoui et al. (2009) measured  $\text{NH}_3$  and  $\text{CO}_2$  concentrations in the headspace of a closed 1 L jar that contained about 150 g (2.5 cm) of previously stored dairy cattle manure. They measured headspace concentrations of  $\text{NH}_3$  and  $\text{CO}_2$  using a photoacoustic spectrometer, with exhaust gas recycled back into the headspace, providing some mixing. They observed an increase in  $\text{NH}_3$  concentration, with a peak after about 30 min, followed by a gradual decline that continued for 15 h. Conversely,  $\text{CO}_2$  increased over the entire period (Fig. 5 in Chaoui et al., 2009). Again, this response is consistent with predictions from our model. The initial increase in  $\text{NH}_3$  concentration can be explained by  $\text{NH}_3$  emission from the surface, exacerbated by an increase in surface pH caused by simultaneous  $\text{CO}_2$  emission. Eventually,  $\text{CO}_2$  emission slowed as  $\text{CO}_2$  species were depleted from the surface and  $\text{CO}_2$  (g) accumulated in the headspace. At some point, the rate of diffusion of  $\text{CO}_2$  species exceeded the rate of emission, leading to a decline in surface pH. This decline in pH translated into a decline in the equilibrium partial pressure of  $\text{NH}_3$  at the manure surface, and resulted in absorption of  $\text{NH}_3$ .

For both of these experiments, values are missing for some model parameters, including total  $\text{CO}_2$  concentrations and mass transfer coefficients. With typical values, our model can qualitatively reproduce the observed trajectories. With adjustment of kinetic rates as well, predicted values come close to measurements, although  $\text{CO}_2$  concentrations tend to be underpredicted. These experiments cannot be used as a robust evaluation of our model, but they do provide further evidence that  $\text{CO}_2$  emission and resulting surface pH changes play a role in  $\text{NH}_3$  emission from

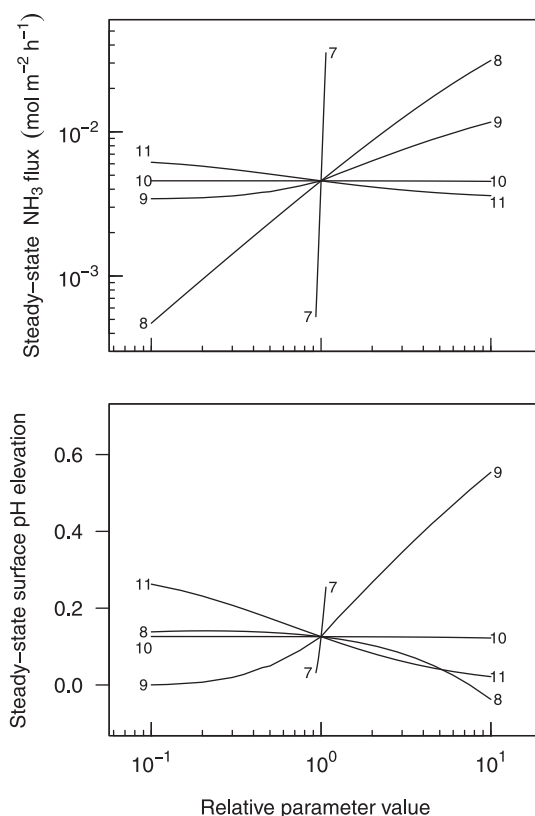


**Fig. 9.** Predicted sensitivity of steady-state  $\text{NH}_3$  flux (top) and surface pH elevation (bottom) to model parameters for manure with a stagnant film at the surface and a bulk solution with a constant composition. Line labels are as in Fig. 6.

manure. A more complete test of our model, and assessment of the importance of the processes included, will require carefully controlled emission measurements from well-characterized manure. Characterization of manure will need to include total  $\text{NH}_3$  and total  $\text{CO}_2$  concentrations, pH, and ideally other important solutes. Ammonia emission can be measured using a wind tunnel or flux chamber. In either case, the mass transfer coefficient of the system should be determined.

Predictions from our model suggest that current models of  $\text{NH}_3$  emission from manure that predict solution speciation from bulk pH measurements are not based on an accurate description of the processes responsible for  $\text{NH}_3$  emission, even when model predictions appear accurate. This is most important for thin layers of manure, where  $\text{CO}_2$  emission was predicted to cause the greatest elevation of surface pH. Since models that include a more accurate representation of important processes ultimately provide more accurate predictions and are more generally applicable than empirical models, such models should be pursued. In some cases, a more accurate model may be useful for predicting the effect of management changes. For example, our model predicts that  $\text{NH}_3$  emission from mixed manure decreases as liquid mixing increases (represented by a decrease in stagnant film thickness) due to increased buffering of surface pH by diffusing  $\text{CO}_2$  species. Blanes-Vidal et al. (2010) also predicted that  $\text{NH}_3$  emission rate would be greater from unmixed than from mixed manure. This interaction may have implications for controlling  $\text{NH}_3$  emission. In preliminary laboratory measurements, we found that  $\text{NH}_3$  flux from diluted dairy manure was almost an order of magnitude greater when left undisturbed over a day than when stirred (Supplementary material). However,  $\text{NH}_3$  depletion over longer periods and development of a surface crust probably confound this difference on

farms. Another unexpected response that our model predicted is that  $\text{NH}_3$  emission from thin layers of manure may exceed emission from thicker layers over short periods of time. Understanding and evaluating these types of interactions requires both measurement and modeling approaches.

Predictions from our model, coupled with our measurements and observations made previously by others show that  $\text{CO}_2$  plays an important role in  $\text{NH}_3$  emission from manure. However, at least three areas need attention in order to better understand  $\text{NH}_3$  emission from manure: fractionation of total  $\text{CO}_2$  in manure, transport of  $\text{CO}_2$  by bubbles, and measurement of  $\text{CO}_2$  hydration/dehydration rates in manure. Precipitated carbonate minerals, which are probably present in manure (Husted et al., 1991), behave differently than aqueous  $\text{CO}_2$  species in their effect on  $\text{NH}_3$  emission; therefore, measurement of manure  $\text{CO}_2$  should distinguish between them. Dissolution or formation of minerals over hours or days may add complexity to  $\text{NH}_3$  emission.

Emission of  $\text{CO}_2$  via bubbles from manure has been discussed by others (Ro et al., 2008; Ni et al., 2009; Blanes-Vidal and Nadimi, 2011). This process may transport  $\text{CO}_2$  to the manure surface, and so moderate the elevation of pH due to  $\text{CO}_2$  emission from the surface in some cases. As discussed above, bubbles also contribute to convective transport of the solution. Simple laboratory experiments that include forced  $\text{CO}_2$  bubbling could provide insight into these processes.

Rates of  $\text{CO}_2$  hydration/dehydration almost certainly play an important role in determining  $\text{NH}_3$  emission rates from manure. These slow hydration/dehydration reactions can be catalyzed by the enzyme carbonic anhydrase. To our knowledge, no measurements of the activity or presence of this enzyme in cattle manure have been made. Ruminants produce carbonic anhydrase in the saliva and rumen epithelium (Jouany, 1991), but the enzyme is probably inactivated in the stomach. Prokaryotes, including both Bacteria and Archaea, also produce isozymes of this enzyme (Smith and Ferry, 2000), and it is therefore likely that some activity is present in cattle manure.

#### 4. Conclusions

Predictions from our model and measurements from simple solutions confirmed that  $\text{CO}_2$  emission influences  $\text{NH}_3$  emission from manure. In our model predictions, carbon dioxide emission generally increased  $\text{NH}_3$  flux by elevating surface pH. For thin stagnant layers, this response occurred under a wide range of conditions. Kinetically-limited reactions moderated this effect, suggesting that equilibrium-based models will tend to over-predict  $\text{NH}_3$  emission in the absence of significant carbonic anhydrase activity. Predicted emission from deep mixed manure showed less dependence on  $\text{CO}_2$  emission, and simpler models, without a speciation component, may be able to capture the response of steady-state  $\text{NH}_3$  flux to parameters for at least some cases. Model predictions demonstrated that manure composition can influence  $\text{NH}_3$  emission in ways not previously recognized. Our model can inform the development of simpler models for estimating  $\text{NH}_3$  emission, and the design of experiments aimed at quantifying processes that influence  $\text{NH}_3$  emission from manure. Future work should address the processes controlling  $\text{CO}_2$  speciation and transport in manure, including  $\text{CO}_2$  minerals, bubble transport, and  $\text{CO}_2$  hydration/dehydration rates. In general, development of more accurate emission models requires that more attention be given to the effects of  $\text{CO}_2$  on  $\text{NH}_3$  emission. Both experimental and modeling approaches are needed to understand the interactions that control  $\text{NH}_3$  emission.

## Acknowledgments

We thank Karl-Heinz Südekum (University of Bonn), Marcus Mau (King's College London), and Ransom Baldwin (USDA-ARS) for providing information on carbonic anhydrases. Jiqin Ni (Perdue University) kindly shared NH<sub>3</sub> and CO<sub>2</sub> emission data. John J. Meisinger (USDA-ARS) provided helpful comments on a draft of this manuscript. We also appreciate the careful reviews and helpful suggestions provided by two anonymous reviewers.

## Appendix. Supplementary material

Supplementary data related to this article can be found online at doi:10.1016/j.atmosenv.2012.01.026.

## References

- Blanes-Vidal, V., Nadimi, E., Sep. 2011. The dynamics of ammonia release from animal wastewater as influenced by the release of dissolved carbon dioxide and gas bubbles. *Atmospheric Environment* 45 (29), 5110–5118.
- Blanes-Vidal, V., Nadimi, E.S., Sommer, S.G., Dec. 2010. A comprehensive model to estimate the simultaneous release of acidic and basic gaseous pollutants from swine slurry under different scenarios. *Chemistry and Ecology* 26, 425–444.
- Blanes-Vidal, V., Sommer, S., Nadimi, E., 2009. Modelling surface pH and emissions of hydrogen sulphide, ammonia, acetic acid and carbon dioxide from a pig waste lagoon. *Biosystems Engineering* 104 (4), 510–521.
- Blunden, J., Aneja, V.P., Overton, J.H., 2008. Modeling hydrogen sulfide emissions across the gas-liquid interface of an anaerobic swine waste treatment storage system. *Atmospheric Environment* 42 (22), 5602–5611.
- Chaoui, H., Montes, F., Rotz, C.A., Richard, T.L., 2009. Volatile ammonia fraction and flux from thin layers of buffered ammonium solution and dairy cattle manure. *Transactions of the ASABE* 52 (5), 1695–1706.
- Clegg, S., Brimblecombe, P., 1989. Solubility of ammonia in pure aqueous and multicomponent solutions. *Journal of Physical Chemistry* 93 (20), 7237–7248.
- Clegg, S.L., Whitfield, M., 1995. A chemical-model of seawater including dissolved ammonia and the stoichiometric dissociation-constant of ammonia in estuarine water and seawater from -2°C to 40°C. *Geochimica et Cosmochimica Acta* 59 (12), 2403–2421.
- EPA, U., 2004. National Emission Inventory—Ammonia Emissions from Animal Husbandry Operations Draft Report. US EPA, Washington DC.
- EPA, U., 2009. National Emissions Inventory (NEI) Air Pollutant Emissions Trends Data. US EPA, Washington DC.
- Galloway, J., Aber, J., Erisman, J., Seitzinger, S., Howarth, R., Cowling, E., Cosby, B., 2003. The nitrogen cascade. *Bioscience* 53 (4), 341–356.
- Genermont, S., Cellier, P., 1997. A mechanistic model for estimating ammonia volatilization from slurry applied to bare soil. *Agricultural and Forest Meteorology* 88 (1–4), 145–167.
- Gungor, K., Karthikeyan, K., 2008. Phosphorus forms and extractability in dairy manure: a case study for wisconsin on-farm anaerobic digesters. *Bioresource Technology* 99 (2), 425–436.
- Hafner, S., Jewell, W., Bisogni, J.J., 2006. Ammonia speciation in anaerobic digesters. In: 2006 ASABE Annual International Meeting Proceedings Portland, OR.
- Hafner, S., Meisinger, J., Mulbry, W., Ingram, S. A pH-based method for measuring gaseous ammonia. *Nutrient Cycling in Agroecosystems*, in press.
- Hafner, S.D., Bisogni, J.J., 2009. Modeling of ammonia speciation in anaerobic digesters. *Water Research* 43 (17), 4105–4114.
- Husted, S., Jensen, L.S., Jørgensen, S.S., Jan. 1991. Reducing ammonia loss from cattle slurry by the use of acidifying additives: the role of the buffer system. *Journal of the Science of Food and Agriculture* 57 (3), 335–349.
- Jouany, J.P., 1991. Rumen Microbial Metabolism and Ruminant Digestion. Editions Quae, Versailles, France.
- Kern, D.M., 1960. The hydration of carbon dioxide. *Journal of Chemical Education* 37, 14–23.
- Kirk, G., Rachhpal-Singh, 1992. Simultaneous transfer across an air–water interface of gases that interact through acid–base reactions. *Atmospheric Environment* 26 (9), 1651–1660.
- Liang, Z., Westerman, P., Arogo, J., 2002. Modeling ammonia emission from swine anaerobic lagoons. *Transactions of the ASABE* 45 (3), 787–798.
- Linstrom, P., Mallard, W. (Eds.), 2011. NIST Chemistry WebBook, NIST Standard Reference Database Number 69. National Institute of Standards and Technology, Gaithersburg, MD. <http://webbook.nist.gov>.
- Liss, P., Slater, P.G., 1974. Flux of gases across air-sea interface. *Nature* 247 (5438), 181–184.
- Martell, A., Smith, R., Motekaitis, R., 2004. Database 46: NIST Critically Selected Stability Constants of Metal Complexes. <http://www.nist.gov/srd/nist46.cfm>.
- Ni, J., Heber, A., Sutton, A., Kelly, D., 2009. Mechanisms of gas releases from swine wastes. *Transactions of the ASABE* 52 (6), 2013–2025.
- Ni, J., Hendriks, J., Vinckier, C., Coenegrachts, J., 2000. A new concept of carbon dioxide accelerated ammonia release from liquid manure in pig house. *Environment International* 26 (1–2), 97–104.
- Plummer, L., Busenberg, E., 1982. The solubilities of calcite, aragonite and vaterite in CO<sub>2</sub>-H<sub>2</sub>O solutions between 0°C and 90°C, and an evaluation of the aqueous model for the system CaCO<sub>3</sub>-CO<sub>2</sub>-H<sub>2</sub>O. *Geochimica et Cosmochimica Acta* 46 (6), 1011–1040.
- R Development Core Team, 2010. R: a Language and Environment for Statistical Computing. <http://www.R-project.org>.
- Ro, K., Szogi, A., Vanotti, M., Stone, K., 2008. Process model for ammonia volatilization from anaerobic swine lagoons incorporating varying wind speeds and gas bubbling. *Transactions of the ASABE* 51 (1), 259–270.
- Schiesser, W.E., 1991. *The Numerical Method of Lines: Integration of Partial Differential Equations*. Academic Press.
- Smith, K., Ferry, J., 2000. Prokaryotic carbonic anhydrases. *FEMS Microbiology Reviews* 24 (4), 335–366.
- Sommer, S., Olesen, J., Christensen, B., 1991. Effects of temperature, wind-speed and air humidity on ammonia volatilization from surface applied cattle slurry. *Journal of Agricultural Science* 117, 91–100.
- Sommer, S.G., Gnermont, S., Cellier, P., Hutchings, N.J., Olesen, J.E., Morvan, T., 2003. Processes controlling ammonia emission from livestock slurry in the field. *European Journal of Agronomy* 19 (4), 465–486.
- Sommer, S.G., Husted, S., 1995a. The chemical buffer system in raw and digested animal slurry. *The Journal of Agricultural Science* 124 (01), 45–53.
- Sommer, S.G., Husted, S., 1995b. A simple model of pH in slurry. *The Journal of Agricultural Science* 124 (03), 447–453.
- Welch, M., Lifton, J., Seck, J., 1969. Tracer studies with radioactive oxygen-15. exchange between carbon dioxide and water. *Journal of Physical Chemistry* 73 (10), 3351–3356.
- Zemaitis, J.F., 1986. *Handbook of Aqueous Electrolyte Thermodynamics: Theory & Application*. Design Institute for Physical Property Data Sponsored by the American Institute of Chemical Engineers, New York, N.Y.